Simvastatin treatment highlights a new role for the isoprenoid/cholesterol biosynthetic pathway in the modulation of emotional reactivity and cognitive performance in rats

Marco Segatto[1], Antonia Manduca[1], Claudio Lecis[1], Pamela Rosso[1], Adam Jozwiak[2], Ewa Swiezewska[2], Sandra Moreno[1], Viviana Trezza[1] and Valentina Pallottini[1]*

[1]Department of Science, University Roma Tre, Viale Marconi, 446 00146 Rome, Italy

[2]Institute of Biochemistry and Biophysics Polish Academy of Sciences, Pawinskiego 5a, 02-106 Warsaw, Poland

* Corresponding author: Valentina Pallottini,

Department of Science, University Roma Tre, Viale Marconi, 446 00146 Rome, Italy

e-mail:valentina.pallottini@uniroma3.it

Tel: +39 06 57336320

Fax: +39 06 57336321

Abbreviated title: **Role of HMGR inhibition in brain functioning**

Keywords: simvastatin, memory, anxiety, RhoA, Rab3, CREB

Abstract

The aim of the present work was to shed light on the role played by the isoprenoid/cholesterol biosynthetic pathway in the modulation of emotional reactivity and memory consolidation in rodents through the inhibition of the key and rate-limiting enzyme 3-hydroxy 3-methylglutaryl Coenzyme A reductase (HMGR) both *in vivo* and *in vitro* with simvastatin.

Three-month-old male Wistar rats treated for 21 days with simvastatin or vehicle were tested in the social interaction, elevated plus-maze, and inhibitory avoidance tasks; after behavioral testing, the amygdala, hippocampus, prefrontal cortex, dorsal and ventral striatum were dissected out for biochemical assays. In order to delve deeper into the molecular mechanisms underlying the observed effects, primary rat hippocampal neurons were used.

Our results show that HMGR inhibition by simvastatin induces anxiogenic-like effects in the social interaction but not in the elevated plus maze test, and improves memory consolidation in the inhibitory avoidance task. These effects are accompanied by imbalances in the activity of specific prenylated proteins, Rab3 and RhoA, involved in neurotransmitter release and synaptic plasticity, respectively. Taken together, the present findings indicate that the isoprenoid/cholesterol biosynthetic pathway is critically involved in the physiological modulation of both emotional and cognitive processes in rodents.

INTRODUCTION

The isoprenoid/cholesterol biosynthetic pathway, also known as mevalonate (MVA) pathway, is one of the most notorious metabolic processes since it leads to the production of cholesterol and other non-sterol isoprenoids which are essential in the induction and the maintenance of several cellular processes. The key enzyme of this pathway is the 3-hydroxy-3-methylglutaryl coenzyme A reductase (HMGR) (Brown and Goldstein, 1980; Segatto *et al*, 2013). The role of MVA pathway is well established in the liver, where a major part of lipid metabolism takes place (Horton, 2002; Pallottini *et al*, 2007; Segatto *et al*, 2013). However this metabolic pathway is ubiquitously expressed in all eukaryotic cells, and recent studies sustain a pivotal role for MVA end-products in the brain. Although the CNS constitutes the 2% of the body weight, it contains about 25% of the total body cholesterol (Pfrieger, 2003; Segatto *et al*, 2013). The majority of cholesterol is present in myelin sheaths and in neuronal membranes, where this lipid fulfills structural and functional tasks. Given the crucial role of cholesterol in regulating different neuronal processes, eukaryotes have developed sophisticated homeostatic mechanisms to preserve cholesterol levels in an optimal range in each brain region (Segatto *et al*, 2013). Thus, alterations in this essential equilibrium could lead to pathological consequences in the CNS, such as Smith-Lemli-Opitz syndrome, Alzheimer's and Niemann-Pick type C diseases (Dietschy and Turley, 2004; Pfrieger, 2003; Segatto *et al*, 2011).

Besides cholesterol, isoprenoid compounds carry out important roles in the CNS. Prenylation, the covalent binding of farnesyl pyrophosphate (FPP) or geranylgeranyl pyrophosphate (GGPP) moieties to proteins, is a crucial post-translational modification for the regulation of protein localization on cell membranes and, in turn, for key cellular processes. Isoprenoids are not only required for protein prenylation, but also constitute the side chain of Coenzyme Q (CoQ) (Matthews *et al*, 1998), whereas dolichols are involved in the N-linked glycosylation of proteins (Trapani *et al*, 2011b).

The essential role of MVA end-products in the CNS physiology is also supported by growing pre-clinical and clinical studies on the pleiotropic effects of statins in the brain. Statins are strong HMGR inhibitors widely prescribed in therapies against hypercholesterolemia and their benefits in preventing atherosclerosis and other cardiovascular diseases are incontrovertible. Recently, it has been reported that high dose statin treatment induces effects in emotional, learning and memory processes (Kilic *et al*, 2012; Douma *et al*, 2011; Baytan *et al*, 2008; While and Keen, 2010). However, the role of the MVA biosynthetic pathway in the modulation of emotional behavior and cognitive performance is still unclear because of the lack of systematic studies on the causal link between the activation of this metabolic pathway and behavioral and cognitive outcomes. As a consequence, the effects exerted by statins in the CNS still remain confusing and unconvincing. Moreover, no data about a low-dose statin treatment is available. A better understanding of these processes could be of great interest towards new pharmacological interventions for CNS disorders. Thus, the aim of the present work was to shed light on the role played by the MVA pathway in the modulation of emotional reactivity and memory consolidation in rodents, through the inhibition by simvastatin of HMGR both *in vivo* and *in vitro*.

MATERIALS AND METHODS

Animals

Three-months-old male Wistar rats (Harlan Nossan, S. Pietro al Natisone, Italy) were housed in groups of two and maintained under controlled temperature (20 ± 1 °C), humidity ($55 \pm 10\%$) and illumination (12/12 h light cycle with lights on at 7.00 a.m.). Food and water were provided *ad libitum*. All procedures involving animal care or treatments were approved by the Italian Ministry of Health and performed in compliance with the guidelines of the US National Institutes of Health (NIH) and the Italian Ministry of Health (n° 231/2012-B, according to D.L. 116/92), the Declaration of Helsinki, the Guide for the Care and Use of Mammals in Neuroscience and

Behavioral Research (National Research Council 2004) and the Directive 2010/63/EU of the European Parliament and of the Council of 22 September 2010 on the protection of animals used for scientific purposes.

Drug Treatment

Simvastatin (Sigma Aldrich, Milan, Italy) was dissolved in a vehicle containing dimethyl sulfoxide - 250 µl/kg body weight of 10% DMSO in sterile H_2O (v/v) - and the dose of 1.5 mg/kg was daily administered by intraperitoneal injections for 3 weeks. Control animals were treated with vehicle only. Immediately after testing, rats were deeply anesthetized using Urethane (1.2 mg/kg) and plasma obtained from blood collected into EDTA (1 mg/ml blood). Subsequently, rats were decapitated and their brains quickly removed. Brain regions of interest (amygdala, hippocampus, prefrontal cortex, dorsal and ventral striatum) were collected and frozen in liquid nitrogen for subsequent biochemical analyses.

Plasma cholesterol analysis

Plasma cholesterol content was estimated by the colorimetric CHOD-POD kit in accordance to the manufacturer's instructions (Assel, Rome, Italy).

Plasma triglycerides analysis

The amount of plasma triglycerides was assessed by using the Triglyceride Quantification Kit in accordance to the manufacturer's instructions (BioVision, Mountain View, CA).

Behavioral tests

The behavioral experiments were performed the day following the last administration of either simvastatin or vehicle. Different groups of rats were used for each behavioral test.

Social interaction test

The social interaction test was performed under dim light conditions in a Plexiglas arena (45 x 45 x 60 cm) with approximately 2 cm of wood shavings covering the floor.

The test consisted in placing two similarly treated animals into the test cage for 10 min, with new sawdust as bedding. The animals in a pair did not differ more than 10 g in body weight; furthermore, they were housed in different cages and that therefore had no previous common social experience from the arrival in our Facility till the day of testing (File, 1980; Trezza *et al*, 2008).

The behavior of the animals was recorded on DVD for subsequent appropriate behavioral analysis carried out by the same observer, who was unaware of animal treatment, using the Observer 3.0 software (Noldus Information Technology B.V., Wageningen, The Netherlands).

The total time spent in active social interaction was obtained as the sum of the time spent in the following behavioral elements scored per 10 min:

– Play-related behaviors: 1. total time spent in pouncing (i.e., when one animal attempts to nose or rub the nape of the neck of its play partner) which is an index of play solicitation; 2. total time spent in pinning (i.e., the most common terminal component of a play bout, in which one animal stands over a supine partner), which is the consummatory measure of play (Panksepp *et al*, 1984; Trezza *et al*, 2010).

– Social behaviors unrelated to play: total time spent in social exploration (sniffing any part of the body of the test partner, including the anogenital area; social grooming; following/chasing).

Elevated plus-maze

The elevated plus-maze test was performed as previously described (Pellow and File, 1986; Trezza *et al*, 2009). Briefly, the rats were individually placed on the central platform of the maze, facing a closed arm, and allowed to freely explore the maze for 5 min.

The 5 min test period was recorded on DVD for subsequent appropriate behavioral analysis carried out by the same observer, unaware of animal treatment, using the Observer 3.0 software (Noldus Information Technology B.V., Wageningen, The Netherlands).

The following parameters were analyzed:

a.   % time spent on the open arms (% TO): (seconds spent on the open arms of the maze/300) × 100;

b.   % open arm entries (% OE): (the number of entries into the open arms of the maze/ number of entries into open + centre + closed arms) × 100;

c.   number of total arm entries (open + closed arm entries).

Inhibitory Avoidance

The inhibitory-avoidance apparatus (Ugo Basile, Comerio, Italy) consisted of a Plexiglas cage with tilting floor, divided by a sliding door into two compartments (22×22×25 cm each). One of the compartments had white walls and was brightly illuminated by a 10-W bulb. The other compartment had black walls and was not illuminated. The tilting floor consisted of bars of stainless steel connected to a source of scrambled shock. The procedure consisted of two sessions, acquisition and retention, that took place on 2 subsequent days (Mereu *et al*, 2003; Campolongo *et al*, 2007). For details see Supplementary Materials and Methods.

Lipid extraction

Lipid extraction from brain regions (amygdala, hippocampus, prefrontal cortex, dorsal striatum and ventral striatum) was assessed by following the previously described protocol (Trapani *et al*, 2011a).

HPLC-UV analysis of isoprenoids

Cholesterol, Coenzyme Q9 (CoQ9), Coenzyme Q10 (CoQ10) and dolichols were analyzed according to the previously described protocol (Tang *et al*, 2001) with modifications. For details see Supplementary Materials and Methods.

Lysate, cytosol and membrane preparation from brain tissue

Lysate and membrane from brain tissue were prepared slightly modifying our previously used protocol (Segatto *et al*, 2011). For details, see Supplementary Materials and Methods.

Synaptic vesicle preparation

Synaptic vesicles were prepared following the protocol described by Huttner et al. (1983) with modifications. Rat brain regions (amygdala, hippocampus, prefrontal cortex, dorsal striatum and ventral striatum) were homogenized in 10 volumes of ice cold HEPES-buffered sucrose (4 mM HEPES, 0.32 M sucrose, 0.001 M PMSF, pH 7.4) with 10 strokes in a glass-Teflon homogenizer. Homogenates were centrifuged at 1,000 g to remove nuclei, intact cells and cell debris (P1 fraction). The supernatant (S1) was spun at 10,000 g for 15 min to yield the crude synaptosomal pellet (P2). The supernatant (S2) was collected and subsequently centrifuged at 100,000 g for 15 min to produce the cytosolic fraction (S2'). The P2 fraction was then resuspended in 10 volumes of HEPES-buffered sucrose and respun at 10,000 g for 15 min to obtain the washed crude synaptosomal fraction (P2'). The resulting pellet was lysed by hypoosmotic shock in 9 volumes of ice cold distilled water plus 0.001 M PMSF and three strokes of a glass-Teflon homogenizer. 4 mM HEPES (pH 7.4) was rapidly added to the lysate which was mixed continuously in a cold room for 30 min to guarantee the total lysis of the sample. The lysate was subsequently centrifuged at 25,000 g for 20 min and the supernatant (S3) was collected and spun at 165,000 g for 2 hours. The pellet of synaptic vesicles was finally solubilized in a sample buffer (0.125M Tris–HCl -pH 6.8- containing 10% SDS, 0.001 M PMSF) and transferred into 1.5 ml Eppendorf tubes. Protein determination was assessed by the method of Lowry et al. (Lowry *et al*, 1951). The synaptic vesicle samples were boiled for 3 min before loading for Western blotting method. In order to obtain an adequate amount of synaptic vesicles, each sample was made up from six brain regions pulled together from six different animals. The protein detection of synaptophysin (synaptic vesicle marker) and α-tubulin (cytosolic marker) verified and confirmed a high degree of purity of the synaptic vesicles (Figure S1).

Rab3 "in vitro" degradation assay

Rab3 degradation assay was performed according to the protocol used by Pallottini et al., (Pallottini *et al*, 2004) with modifications. For details see Supplementary Materials and Methods.

Hippocampal neuron primary cultures and drug treatment

Primary hippocampal neurons were isolated and cultured according to the previously described protocol (Oh *et al*, 2006). For details see Supplementary Materials and Methods.

Western blotting analysis

Western blot method was performed slightly modifying the protocol described by Trapani et al. (Trapani *et al*, 2011a) by using the following antibodies: LDLr ab30532 (Abcam); SREBP-2 ab28482 (Abcam); NeuN A60 (Chemicon); GFAP 134B1 (Synaptic Systems); Rab3 G-1, CREB, p-CREB, H-Ras M90, RhoA 26C4, Akt1 B-1, RhoGDI A-20, RabGDI (V-20)-R, synaptophysin H-93, caveolin N-20 (Santa Cruz Biotechnology); p-Akt 193H12 (Cell Signaling). For details see the Supplementary Materials and Methods.

Immunohistochemistry

Immunohistochemical staining of p-CREB and PSD-95 was performed on sagittal brain sections of simvastatin- and vehicle-treated animals according to the previously used protocols (Moreno *et al*, 1995; Fanelli *et al*, 2013). For details see Supplementary Materials and Methods.

Statistical analysis

Data obtained from behavioral tests are expressed as means ± SEM (standard error of the mean); data derived from the analysis of biochemical results are expressed as means ± SD (standard deviation). Data were analyzed with unpaired Student's *t* test or with one-way analysis of variance (ANOVA) followed by Dunnett post-test. Values of $P < 0.05$ were considered to indicate a significant difference. Statistical analysis was performed using GRAPHPAD INSTAT3 (GraphPad, La Jolla, CA, USA) for Windows.

RESULTS

Systemic effects of HMGR inhibition on lipid metabolism

The inhibition of HMGR, and in turn the reduction in MVA end-products formation, leads to a homeostatic response which determines the increase of the Low Density Lipoprotein (LDL) receptor family members through the enhancement of their transcription and translocation onto cell membranes, subsequently reducing the amount of plasma lipids (Jones *et al*, 1998). Thus, the efficacy of the pharmacological treatment was checked by estimating plasma cholesterol and triglycerides. As shown in Table S1, both cholesterol ($t_{34} = 3,606$, p = 0,001) and triglycerides ($t_{34} = 4,562$, p > 0,0001) significantly decreased after simvastatin treatment (18% and 32%, respectively). Nevertheless, similar body weight of simvastatin- and vehicle-treated rats was observed, indicating that HMGR inhibition failed to induce changes in the basal metabolism of the animals (data not shown).

Effects of HMGR inhibition on emotional reactivity and cognitive performance

To evaluate the potential role of MVA pathway inhibition by simvastatin in the modulation of emotional reactivity, rats were tested in the social interaction and elevated plus maze tests, two validated animal methods to evaluate anxiety in rodents.

Chronic simvastatin treatment decreased the total time spent in active social interaction compared with vehicle-treated rats ($t_{18} = 4,123$, *p* < 0,001; Figure 1a), expressed as the sum of the time spent in play-related behaviors ($t_{18} = 3,386$, *p* = 0,003; figure not shown) and in social behaviors unrelated to play ($t_{18} = 2,390$, *p* = 0,028; figure not shown). In contrast, the percentage of time spent in the open arms ($t_{19} = -1,349$, *p* = 0,193; Figure 1b), the percentage of open entries ($t_{19} = -1,062$, *p* = 0,302; Figure 1c) and the total arm entries ($t_{19} = 1,768$, *p* = 0,093; Figure 1d) evaluated in the elevated plus-maze test were unaffected by the pharmacological inhibition of HMGR.

To investigate whether MVA pathway has a role in the modulation of memory consolidation, rats were tested in the inhibitory avoidance task. Chronic simvastatin treatment had no effect on the

approach latencies during the acquisition trial (t_{17} = -0,620, p = 0,544; Figure 1e); however, it caused a statistically significant improvement in 24-hours retention performance (t_{17} = -2,245, p = 0,038; Figure 1f). This effects was not secondary to drug-induced hypersensivity to the electrical shock delivered during the acquisition trial, since simvastatin- and vehicle-treated rats did not differ in the response to the aversive stimulus during the acquisition trial (t_{17} = -0,204, p = 0,841; Figure 1g).

Simvastatin efficacy and tolerance in the CNS

Evidence for the drug efficacy in the CNS were given by checking the levels of the active nuclear fraction of the transcription factor SREBP-2 (nSREBP-2) and the subsequent increase in LDL receptor (LDLr), that are induced by a compensative response due to intracellular cholesterol decrease (Brown and Goldstein, 1997; Trapani *et al*, 2011a). The biochemical analysis were mainly carried out on amygdala, hippocampus, prefrontal cortex, dorsal striatum and ventral striatum, whose interplay is deeply involved in the modulation of anxiety, memory and learning (Mathew *et al*, 2001; LaBar and Cabeza, 2006). Our results showed that HMGR inhibition by chronic simvastatin treatment induced a classical feedback response, which led to a strong increase of the active nSREBP-2 in all the brain regions analyzed (amygdala: t_{10} = 2,139, p = 0,0291; hippocampus: t_{10} = 2,434, p = 0,0176; prefrontal cortex: t_{10} = 2,590, p = 0,0135; dorsal striatum: t_{10} = 2,045, p = 0,034; ventral striatum: t_{10} = 2,637, p = 0,0124; Figure 2a). HMGR inhibition was also supported by the subsequent and the contributory increase in LDLr expression (amygdala: t_{10} = 2,263, p = 0,0236; hippocampus: t_{10} = 2,057, p = 0,0334; prefrontal cortex: t_{10} = 1,933, p = 0,0410; dorsal striatum: t_{10} = 1,909, p = 0,0427; ventral striatum: t_{10} = 3,969, p = 0,0013; Figure 2b). Moreover, the direct proof of the pharmacological inhibition was also given by assessing HMGR activity (amygdala: t_8 = 7,694, p < 0,0001; hippocampus: t_8 = 12,66, p < 0,0001; prefrontal cortex: t_8 = 7,259, p < 0,0001; dorsal striatum: t_8 = 4,934, p = 0,0011; ventral striatum: t_8 = 5,092, p = 0,0009; Figure S2a) which was reduced in all the analyzed brain areas.

Once simvastatin efficacy was ascertained, we focused on the potential toxic effects exerted by HMGR inhibition on different brain areas. Protein levels of the neuronal marker NeuN (amygdala: $t_{10} = 1,627$, p = 0,0674; hippocampus: $t_{10} = 0,9974$, p = 0,1710; prefrontal cortex: $t_{10} = 1,271$, p = 0,1162; dorsal striatum: $t_{10} = 5,005$, p = 0,3138; ventral striatum: $t_{10} = 0,8166$, p = 0,2166; Figure 2c) and of the astrocyte marker GFAP (amygdala: $t_{10} = 0,5949$, p = 0,4769; hippocampus: $t_{10} = 1,614$, p = 0,0688; prefrontal cortex: $t_{10} = 1,358$, p = 0,1022; dorsal striatum: $t_{10} = 0,8068$, p = 0,2193; ventral striatum: $t_{10} = 0,7905$, p = 0,2238; Figure 2d) were unchanged in the examined brain areas. The analysis of cleaved caspase-3 also showed that the protein levels of this executive caspase were unaffected by simvastatin treatment (amygdala: $t_{10} = 0,5627$, p = 0,2930; hippocampus: $t_{10} = 0,06597$, p = 0,4744; prefrontal cortex: $t_{10} = 0,8944$, p = 0,1961; dorsal striatum: $t_{10} = 0,7460$, p = 0,2364; ventral striatum: $t_{10} = 0,06921$, p = 0,4731; Figure S2b).

Effect of simvastatin on cholesterol, dolichols and CoQs

A prospective perturbation in MVA pathway end-products induced by HMGR inhibition could be at the root of the behavioral and cognitive effects observed *in vivo*.

Thus, lipid estimation was performed in order to evaluate the effect of simvastatin on the main sterol and non-sterol compounds. As observable in Table 1, tissue cholesterol (amygdala: $t_7 = 0,2031$, p = 0,8448; hippocampus: $t_8 = 0,3502$, p = 0,7352; prefrontal cortex: $t_8 = 0,4874$, p = 0,6391; dorsal striatum: $t_7 = 1,556$, p = 0,1636; ventral striatum: $t_6 = 0,5193$, p = 0,6221), coenzyme Q9 (CoQ9) (amygdala: $t_6 = 0,1524$, p = 0,8838; hippocampus: $t_8 = 0,04377$, p = 0,9662; prefrontal cortex: $t_8 = 1,211$, p = 0,2605; dorsal striatum: $t_8 = 1,623$, p = 0,1433; ventral striatum: $t_5 = 0,2318$, p = 0,8259), coenzyme Q10 (CoQ10) (amygdala: $t_6 = 0,06480$, p = 0,9504; hippocampus: $t_8 = 1,301$, p = 0,2294; prefrontal cortex: $t_8 = 1,294$, p = 0,2319; dorsal striatum: $t_8 = 1,440$, p = 0,1879; ventral striatum: $t_5 = 0,2467$, p = 0,8149), and dolichol (amygdala: $t_8 = 1,805$, p = 0,1087; hippocampus: $t_8 = 0,007556$, p = 0,9942; prefrontal cortex: $t_8 = 0,9631$, p = 0,3637; dorsal striatum: $t_8 = 0,2134$, p =

0,8363; ventral striatum: $t_6 = 0,8525$, $p = 0,4266$) were not affected by HMGR inhibition among the brain regions analyzed.

Prenylated protein involved in synaptic vesicle release: Rab3 determination

Simvastatin treatment could also induce a down-regulation in the activity of small GTPases by affecting their prenylation. For the pivotal role in neurotransmitter release, Rab3 protein localization was analyzed. Rab3 fraction associated with the synaptic vesicle membranes was strongly reduced in the hippocampus ($t_2 = 3,675$, $p = 0,0334$; Figure 3a) and the prefrontal cortex ($t_2 = 7,178$, $p = 0,0094$; Figure 3a) after chronic simvastatin treatment, while no differences in the protein localization were observable in amygdala ($t_2 = 1,028$, $p = 0,4120$; Figure 3a), dorsal striatum ($t_2 = 1,592$, $p = 0,1262$; Figure 3a) and ventral striatum ($t_2 = 0,3310$, $p = 0,3860$; Figure 3a). It is well accepted that membrane versus cytoplasm localization of Rab3, and other prenylated small GTPases in general, mirrors the prenylation status and, as a consequence, the activity of the protein of interest (Seasholtz *et al*, 1999; Homma *et al*, 2008). Thus the amount of Rab3 active fraction was expressed as the membrane:cytosol ratio. To further assess Rab prenylation, co-immunoprecipitation experiments between RabGDI and Rab3 were performed on cytosolic fractions. The level of prenylated Rab3 is strongly reduced in the hippocampus ($t_4 = 13,15$, $p = 0,0002$, Figure S3a) and the prefrontal cortex ($t_4 = 6,759$, $p = 0,0025$, Figure S3b) of simvastatin-treated rats. Moreover, the total amount of RabGDI both in the hippocampus ($t_6 = 1,422$, $p = 0,2048$, Figure S3c) and the prefrontal cortex ($t_6 = 0,8552$, $p = 0,4253$, Figure S3d) did not change between the two experimental groups. The lack of the concurrent accumulation of unprenylated Rab3 in the cytosolic fraction (generally a typical phenomenon observed after statin administration) is in line with the results obtained by other research groups, who demonstrated that, under specific conditions, some prenylated proteins could have a shorter half-life compared with the membrane-bound forms (Haklai *et al*, 1998; Indolfi *et al*, 2002). To test this hypothesis, an "in vitro" degradation assay of Rab3 was performed. The results show that Rab3 was more susceptible to

13

degradational events in the hippocampus and the prefrontal cortex, while no differences were detectable between the two experimental groups in the other brain regions (Figure 3b).

Prenylated proteins involved in long-term potentiation: Ras and RhoA determination

The enhanced memory consolidation in a 24h inhibitory avoidance task could correlate with changes in long-term potentiation (LTP). Thus, prenylated proteins such as Ras and RhoA, involved in the modulation of this form of synaptic plasticity (Mazzucchelli and Brambilla, 2000; Rex *et al*, 2009) were evaluated. HMGR inhibition did not induce any statistically significant modification in Ras translocation (amygdala: $t_{10} = 0,2375$, p = 0,4085; hippocampus: $t_{10} = 0,2929$, p = 0,3881; prefrontal cortex: $t_{10} = 0,2798$, p = 0,3927; dorsal striatum: $t_{10} = 0,01021$, p = 0,4960; ventral striatum: $t_{10} = 0,1791$, p = 0,4307; Figure 4a), whereas it strongly reduced the active membrane-bound form of RhoA in the amygdala ($t_{10} = 2,701$, p = 0,0111; Figure 4b) and the hippocampus ($t_{10} = 2,601$, p = 0,0132; Figure 4b), with the contributory build-up of the protein in the cytosol. On the contrary, no differences were observable in the prefrontal cortex ($t_{10} = 0,2867$, p = 0,3901; Figure 4b), the dorsal striatum ($t_{10} = 1,442$, p = 0,0899; Figure 4b) and the ventral striatum ($t_{10} = 0,2531$, p = 0,4026; Figure 4b). As for Rab3, co-immunoprecipitation experiments highlighted a reduction in RhoA/RhoGDI complexes in both the amygdala ($t_4 = 6,188$, p = 0,0035, Figure S4a) and the hippocampus ($t_4 = 6,636$, p = 0,0027, Figure S4b), without showing any change in RhoGDI protein content (amygdala: $t_6 = 1,493$, p = 0,1860, Figure S4c; hippocampus: $t_6 = 0,5134$, p = 0,6260, Figure S4d). In addition, the reduction in RhoA translocation to the membrane was accompanied by a marked and significant increase in Akt activation state in both the amygdala ($t_{10} = 2,726$, p = 0,0107; Figure 4c) and the hippocampus ($t_{10} = 2,724$, p = 0,0107; Figure 4c), whereas no differences are detectable in the prefrontal cortex ($t_{10} = 1,365$, p = 0,1010; Figure 4c), the dorsal striatum ($t_{10} = 0,3652$, p = 0,3613; Figure 4c) and the ventral striatum ($t_{10} = 0,1979$, p = 0,4236; Figure 4c). Similar results were also obtained from cell cultures. In primary rat hippocampal neurons, simvastatin treatment reproduced the reduction in RhoA active fraction observed *in vivo*, as demonstrated from

the decrease in the membrane:cytosol ratio ($F_{(6, 21)} = 4,016$, $p = 0,0078$). The supplementation of the medium with either MVA (the direct product of HMGR) or geranylgeraniol (GG, one of the MVA pathway products and the substrate for RhoA prenylation) completely reversed the effect of the pharmacological inhibition of HMGR. On the other hand, the administration of MVA, GG and Rho kinase (ROCK) inhibitor hydroxyfasudil (HF) alone did not cause any effect in the protein translocation as expected (figure 5a). The estimation of Akt protein levels in primary neuronal culture strongly suggests that Akt phosphorylation was dependent on RhoA inhibition by simvastatin, as the co-administration of MVA and GG completely restored the basal levels of Akt activation state ($F_{(6, 21)} = 37,02$, $p < 0,0001$). HF-mediated inhibition of ROCK, the main downstream effector of RhoA, further support this hypothesis by mimicking the effect of simvastatin through the induction of Akt phosphorylation (Figure 5b). Moreover, Akt activation induced a significant increase in the phosphorylation of the transcription factor CREB ($F_{(6, 21)} = 4,849$, $p = 0,003$; Figure 5c).

Immunohistochemical analyses

Morphological analysis of brains from either simvastatin- or vehicle-treated rats revealed good preservation of structures and overall normal cytoarchitecture. Immunohistochemical localization of p-CREB showed wide neuronal distribution in the hippocampal formation of both treated and control groups. Immunostaining was mainly seen in the nucleus of pyramidal cells in CA1-CA3 fields and of granule cells in DG. Also, mossy cells in the hylus were especially immunoreactive. Consistent with Western blot results obtained from primary hippocampal neuron cultures, remarkably higher immunostaining intensity throughout the hippocampus was detected in simvastatin-treated brains, as compared to their untreated counterparts (Figure 6a). PSD-95 also immunolocalized to pyramidal cell layer of CA1-CA3, to granule neurons of DG, and to hylar mossy neurons. However, at difference with p-CREB immunohistochemistry, the staining intensity

was comparable between the two experimental conditions, not being affected by simvastatin treatment (Figure 6b).

DISCUSSION

The present study was performed to provide a deeper understanding of CNS functional consequences following the pharmacological inhibition of the isoprenoid/cholesterol biosynthetic pathway in rodents. To this aim HMGR, the key and rate-limiting enzyme of this pathway, was inhibited in rats by chronic treatment with simvastatin, a powerful HMGR inhibitor which is able to cross the blood brain barrier because of its lipophilic properties (Saheki *et al*, 1994). To analyze the biological role of MVA pathway on rat emotionality, we performed two of the most popular animal tests of anxiety currently used: the social interaction and the elevated plus maze tests (File and Hyde, 1978; File, 1980; Pellow *et al*, 1985; Pellow *et al*, 1986). Chronic simvastatin treatment at a low dose induced a significant decrease in the total time spent in active social investigation in the social interaction test, whereas no significant differences were observed in the elevated plus maze test. Although both the elevated plus maze and the social interaction tests are two validated animal models to measure anxiety-like behaviors in rodents (File, 1980; File and Seth, 2003; Pinheiro *et al*, 2007; Pellow *et al*, 1986), it has been suggested that these tests evoke different states of anxiety in the laboratory animal (Gonzales *et al*, 1996; File, 1992) mediated by different neurobiological pathways (Cheeta *et al*, 2000; File *et al*, 2000; File *et al*, 2004) and thus they could have different sensitivity to simvastatin treatment. Specifically, it has been suggested that the elevated plus maze test mimics a state of generalized anxiety, since it produces an approach/avoidance conflict because the animal is exposed to a novel situation that supposedly creates a conflict between the motivation to explore the environment and an unconditioned fear of novelty (File *et al*, 2004), and this may be the underlying mechanism rendering the elevated plus maze test sensitive to anxiolytic-like drugs

(Handley and McBlane, 1993; Pinheiro *et al*, 2007). On the other hand, in the social interaction test, the variable is the time spent by pairs of male rats in active social interaction and one rat influences the behavior of the other; in fact, when pairs of male rats are placed in a situation in which neither one has established its territory, they engage in active social interaction (File *et al*, 1978). Nevertheless, the social interaction test is also sensitive to a number of environmental and physiological factors such as test conditions (light level and familiarity to the test arena) that can affect anxiety mimicking a state of anxiety most similar to that experienced in generalized anxiety disorder (File, 1980; File *et al*, 2003). Furthermore, our results showed that the pharmacological modulation of MVA pathway end-products is also involved in the modulation of memory consolidation of aversive experiences; in particular, HMGR inhibition by simvastatin treatment led to a specific enhancement of the consolidation phase of the memory process, since the approach latency, measured during the first day of the test, did not differ between the two experimental groups. Our results also corroborate with existing and recently published data, showing that a higher dose of simvastatin (10 mg/kg) resulted in improved memory performance in the passive avoidance test (Douma *et al*, 2011). Even though it was demonstrated that simvastatin induces apoptosis in neurons and astrocytes (Marz *et al*, 2007), the drug, at a dose of 1.5 mg/kg, did not cause any cell loss as observable by the unchanged levels of NeuN, GFAP and of the executive caspase-3, excluding that potential neurotoxic effects exerted by simvastatin could be responsible for the behavioral outcomes observed in the current study. The lack of toxic effects could be explained by the low dose of simvastatin used in the present study. In addition, the safety in terms of necrosis and/or apoptosis of this chronic pharmacological treatment was also demonstrated in our previous work (Trapani *et al*, 2011a). The estimation of tissue cholesterol, dolichol and CoQs through HPLC analyses also excluded the involvement of these end-products in the onset of the behavioral and cognitive changes. The lack of any variation in the amount of these isoprenoids following HMGR inhibition is not surprising if it is considered that they possess very long half-lives in the brain

(Andersson *et al*, 1999). Thus, a 3-weeks chronic simvastatin treatment, at the dose used in the our study, might not be able to impair the physiological levels of cholesterol, dolichol, CoQ9 and CoQ10 in the rat brain areas taken into consideration. On the opposite, membrane-bound Rab3 in the synaptic vesicle fraction, which corresponds to the active fraction of the protein, resulted to be strongly decreased in both the hippocampus and the prefrontal cortex after chronic HMGR inhibition. It is well known that Rab and Rho proteins require prenylation for membrane association and for binding to GDIs. GDIs hold prenylated proteins in the cytosol, acting not only as passive regulators of GTPase activity, but also preventing their degradation (Boulter and Garcia-Mata, 2010; Mohamed *et al*, 2012). GDI capture of membrane-bound Rabs could be physically prevented by modifications in cholesterol content within the membranes (Ganley and Pfeffer, 2006). Even though the amount of cholesterol into membranes was not evaluated in this work, GDI capture of prenylated Rab3 in cytosolic fractions excluded potential interferences of membrane cholesterol in RabGDI/Rab3 interaction, suggesting that the deregulation in Rab3 subcellular distribution is due, at least in part, to an impairment in Rab3 prenylation induced by HMGR inhibition. Moreover, Rab3 seem to be more susceptible to degradational events both in the hippocampus and the prefrontal cortex of simvastatin-treated rats. These findings lead us to hypothesize that the lack of prenylation could impair Rab3/RabGDI interaction in the cytosol, thus preventing the role of RabGDI in protecting Rab proteins from degradation. Although there is a conflicting evidence in literature about the modulation of the specific synaptic mechanisms, it is clear and well defined that Rab3 carries out important physiological roles in neurotransmitter release at a late step during the synaptic vesicle exocytosis (Geppert and Sudhof, 1998). Perturbations in Rab3 activity have already been established. For instance, deregulations in Mss4 (mammalian suppressor of Sec4), a regulator of Rab3 activity, are strongly linked to impairments in neurotransmitter release and to the appearance of neurodegenerative and psychological disorders in rodents such as depressive-like syndromes (Andriamampandry *et al*, 2002; Baskys *et al*, 2007; Blaveri *et al*). Given the important

role of the hippocampus and the prefrontal cortex in the modulation of anxiety (Whitton and Curzon, 1990; Christianson *et al*, 2009), the decrease in Rab3 active fraction in both the brain regions as a molecular consequence of HMGR inhibition, could be related to an impairment in the social behavior observed in the social interaction test and could represent a good explanation of the MVA pathway-related molecular mechanism underlying the social anxiety-related behavior observed in our study.

Besides the reduction in membrane-bound Rab3 protein levels, the role of MVA pathway in emotional memory consolidation could be strongly dependent on the modulation of prenylated proteins which are crucial for the induction and the maintenance of LTP. In particular, a strong and statistically significant decrease in RhoA active fraction was observed in the amygdala and the hippocampus. As for Rab3, additional experiments based on RhoA/RhoGDI interaction further support the previous finding, indicating that the reduced amount of RhoA is the consequence of a defect in prenylation caused by HMGR pharmacological inhibition. Among Rho GTPases, RhoA has been implicated in key neurobiological processes, integrating extracellular and intracellular molecular signals to orchestrate refined and coordinated changes in gene expression and actin cytoskeleton, essential prerequisites for the neurite outgrowth and the modulation of synaptic connectivity (Gopalakrishnan *et al*, 2008; Lingor *et al*, 2007). For these reasons, it is not surprising that RhoA activity has been deeply related to the onset of developmental disabilities such as mental retardation (Ramakers and Storm, 2002). Since RhoA is also considered a negative regulator of Akt, whose phosphorylation, and in turn activation, is a key and triggering event for LTP induction and consequent memory retention (Ming *et al*, 2002; Sui *et al*, 2008), Akt protein levels and phosphorylation state were analyzed. In the present work, the reduction in membrane-bound RhoA is accompanied by a sustained Akt activation. In order to fully confirm the causality between HMGR activity, RhoA activation and Akt phosphorylation, an additional experiment was performed on cell culture. To this aim, primary hippocampal neurons were chosen as experimental

model in order to avoid the well-known incapability of some used compounds (*e.g.* mevalonate) to cross the blood brain barrier *in vivo* (Popjak *et al*, 1977). The rescue experiment performed on primary hippocampal neurons demonstrated that the modulation of Akt is strictly dependent on RhoA/ROCK pathway, whose activation could be heavily affected by HMGR inhibition. A role of Akt in the modulation of cognitive performances in rodents has already been proposed, as it is able to induce LTP and other synaptic plasticity phenomena in both the amygdala and the hippocampus (Opazo *et al*, 2003; Sui *et al*, 2008; Lin *et al*, 2008). Akt could promote these processes, at least in part, by activating the nuclear factor CREB (Du and Montminy, 1998). Indeed, CREB-dependent gene transcription appears to be an essential component of long-term memory formation (Silva *et al*, 1998). Our data strengthen this possibility, as Akt activation is followed by an increased CREB phosphorylation in simvastatin- and HF-treated hippocampal neurons. The results obtained from hippocampal cell cultures are further sustained by p-CREB immunostaining, which is particularly positive in the hippocampus of simvastatin-treated rats if compared with vehicle ones. On the contrary no differences, in terms of immunoreactivity, were detectable in PSD-95. The obtained results are in agreement with other recent published data, which demonstrated that chronic simvastatin treatment restores the expression of the learning- and memory-related genes c-Fos and Egr-1 without inducing any modulation in the classical synaptic markers synaptophysin and PSD-95 (Tong *et al*, 2012). Moreover, considering that c-Fos and Egr-1 are downstream of CREB, our findings support the hypothetical model on cognition effects induced by simvastatin proposed by Tong and colleagues (2012). However, we cannot exclude that perturbations in cytoskeleton remodeling following HMGR inhibition, and in turn RhoA inactivation, could contribute, together with Akt induction, to the enhancement of the consolidation of aversive memories. Considering the divergences in the brain regional metabolism, it is possible to speculate that each brain area can be considered as a unique structure with a specific cellular context, able to react in a different manner to the same stimulus (Segatto *et al.,* 2013). Also in this case, despite the generalized influence on

mevalonate pathway in the CNS, it is clear that simvastatin treatment selectively affected prenylated proteins in specific brain regions. Different effects of HMGR inhibition in dependence on the brain area taken into consideration have already been reported (Wang *et al*, 2006). Thus, the selective effects of simvastatin treatment in reducing the amount of Rab3 and RhoA active fractions observed in this study could be influenced by differences in metabolism, function, turnover or relative abundance of specific prenylated proteins in each brain region.

Despite the involvement of Rab3 and RhoA, other cellular mechanisms not evaluated in this work could contribute to the behavioral and cognitive outcomes induced by simvastatin. Growing evidence supports the hypothesis that statins could lead to brain effects, acting through pleiotropic mechanisms (Sierra *et al*, 2011). For instance, previous works identified changes in plasma cholesterol with the onset of mood/anxiety disorders and the modulation of memory performance (Peter *et al*, 2002; Henderson *et al*, 2003; Granholm *et al*, 2008). Even though the biological significance of these connections is not widely accepted and remains to be clarified because of the presence of contradictory data (Papakostas *et al*, 2004; Taylor *et al*, 2011 ; Reitz *et al*, 2005), we cannot exclude that changes in plasma lipids, also observed in our work, could have a role in the functional effects exerted by simvastatin administration. Moreover, a very recent paper showed that the enhancement of the autophagic flux alleviates memory deficits in a transgenic mouse model of AD (Li *et al*, 2013) . Since statins induce autophagy in different cell types (Wei *et al*, 2013; Parikh *et al*, 2010), it is possible that a potential modulation of this process could participate, together with the alterations highlighted in this work, in the increased memory consolidation observed in simvastatin-treated rats.

In summary, these findings indicate that the modulation of the isoprenoid/cholesterol biosynthetic pathway is critically involved in the physiological modulation of both emotional and cognitive processes in rodents (Figure S5). Even though our results provide some hints for the mechanisms of action of statins in the CNS, more efforts should be done in order to better understand their

pleiotropic molecular effects in the CNS. Thus, the present work sets the stage for a future deeper understanding of the effects induced by simvastatin, which could be useful to better define the emerging and tight connection between MVA pathway and brain physiopathology.

Supplementary information is available at the *Neuropsychopharmacology* website.

Conflict of interest: Authors declare no conflict of interest

References

Andersson HC, Frentz J, Martinez JE, Tuck-Muller CM, Bellizaire J (1999). Adrenal insufficiency in Smith-Lemli-Opitz syndrome. *Am J Med Genet* **82**(5): 382-384.

Andriamampandry C, Muller C, Schmidt-Mutter C, Gobaille S, Spedding M, Aunis D*, et al* (2002). Mss4 gene is up-regulated in rat brain after chronic treatment with antidepressant and down-regulated when rats are anhedonic. *Mol Pharmacol* **62**(6): 1332-1338.

Baskys A, Bayazitov I, Zhu E, Fang L, Wang R (2007). Rab-mediated endocytosis: linking neurodegeneration, neuroprotection, and synaptic plasticity? *Ann N Y Acad Sci* **1122**: 313-329.

Baytan SH, Alkanat M, Okuyan M, Ekinci M, Gedikli E, Ozeren M*, et al* (2008). Simvastatin impairs spatial memory in rats at a specific dose level. *Tohoku J Exp Med* **214**(4): 341-349.

Blaveri E, Kelly F, Mallei A, Harris K, Taylor A, Reid J*, et al* (2010). Expression profiling of a genetic animal model of depression reveals novel molecular pathways underlying depressive-like behaviours. *PLoS One* **5**(9): e12596.

Boulter E, Garcia-Mata R (2010). RhoGDI: A rheostat for the Rho switch. *Small GTPases* **1**(1): 65-68.

Brown MS, Goldstein JL (1980). Multivalent feedback regulation of HMG CoA reductase, a control mechanism coordinating isoprenoid synthesis and cell growth. *J Lipid Res* **21**(5): 505-517.

Brown MS, Goldstein JL (1997). The SREBP pathway: regulation of cholesterol metabolism by proteolysis of a membrane-bound transcription factor. *Cell* **89**(3): 331-340.

Campolongo P, Trezza V, Cassano T, Gaetani S, Morgese MG, Ubaldi M*, et al* (2007). Perinatal exposure to delta-9-tetrahydrocannabinol causes enduring cognitive deficits associated with alteration of cortical gene expression and neurotransmission in rats. *Addict Biol* **12**(3-4): 485-495.

Cheeta S, Kenny PJ, File SE (2000). Hippocampal and septal injections of nicotine and 8-OH-DPAT distinguish among different animal tests of anxiety. *Prog Neuropsychopharmacol Biol Psychiatry* **24**(7): 1053-1067.

Christianson JP, Thompson BM, Watkins LR, Maier SF (2009). Medial prefrontal cortical activation modulates the impact of controllable and uncontrollable stressor exposure on a social exploration test of anxiety in the rat. *Stress* **12**(5): 445-450.

Dietschy JM, Turley SD (2004). Thematic review series: brain Lipids. Cholesterol metabolism in the central nervous system during early development and in the mature animal. *J Lipid Res* **45**(8): 1375-1397.

Douma TN, Borre Y, Hendriksen H, Olivier B, Oosting RS (2011). Simvastatin improves learning and memory in control but not in olfactory bulbectomized rats. *Psychopharmacology (Berl)* **216**(4): 537-544.

Du K, Montminy M (1998). CREB is a regulatory target for the protein kinase Akt/PKB. *J Biol Chem* **273**(49): 32377-32379.

Fanelli F, Sepe S, D'Amelio M, Bernardi C, Cristiano L, Cimini A*, et al* (2013). Age-dependent roles of peroxisomes in the hippocampus of a transgenic mouse model of Alzheimer's disease. *Mol Neurodegener* **8**: 8.

File SE (1980). The use of social interaction as a method for detecting anxiolytic activity of chlordiazepoxide-like drugs. *J Neurosci Methods* **2**(3): 219-238.

File SE (1992). Usefulness of animal models with newer anxiolytics. *Clin Neuropharmacol* **15 Suppl 1 Pt A**: 525A-526A.

File SE, Cheeta S, Kenny PJ (2000). Neurobiological mechanisms by which nicotine mediates different types of anxiety. *Eur J Pharmacol* **393**(1-3): 231-236.

File SE, Hyde JR (1978). Can social interaction be used to measure anxiety? *Br J Pharmacol* **62**(1): 19-24.

File SE, Lippa AS, Beer B, Lippa MT (2004). Animal tests of anxiety. *Curr Protoc Neurosci* **Chapter 8**: Unit 8 3.

File SE, Seth P (2003). A review of 25 years of the social interaction test. *Eur J Pharmacol* **463**(1-3): 35-53.

Ganley IG, Pfeffer SR (2006). Cholesterol accumulation sequesters Rab9 and disrupts late endosome function in NPC1-deficient cells. *J Biol Chem* **281**(26): 17890-17899.

Geppert M, Sudhof TC (1998). RAB3 and synaptotagmin: the yin and yang of synaptic membrane fusion. *Annu Rev Neurosci* **21**: 75-95.

Gonzales R, Bungay PM, Kilanmaa K, Samson HH, Rosselti ZL (1996). In vivo links between neurochemistry and behavioral effects of ethanol. *Alcohol Clin Exp Res* **20**(8 Suppl): 203A-209A.

Gopalakrishnan SM, Teusch N, Imhof C, Bakker MH, Schurdak M, Burns DJ*, et al* (2008). Role of Rho kinase pathway in chondroitin sulfate proteoglycan-mediated inhibition of neurite outgrowth in PC12 cells. *J Neurosci Res* **86**(10): 2214-2226.

Granholm AC, Bimonte-Nelson HA, Moore AB, Nelson ME, Freeman LR, Sambamurti K (2008). Effects of a saturated fat and high cholesterol diet on memory and hippocampal morphology in the middle-aged rat. *J Alzheimers Dis* **14**(2): 133-145.

Haklai R, Weisz MG, Elad G, Paz A, Marciano D, Egozi Y*, et al* (1998). Dislodgment and accelerated degradation of Ras. *Biochemistry* **37**(5): 1306-1314.

Handley SL, McBlane JW (1993). An assessment of the elevated X-maze for studying anxiety and anxiety-modulating drugs. *J Pharmacol Toxicol Methods* **29**(3): 129-138.

Henderson VW, Guthrie JR, Dennerstein L (2003). Serum lipids and memory in a population based cohort of middle age women. *J Neurol Neurosurg Psychiatry* **74**(11): 1530-1535.

Homma N, Nagaoka T, Karoor V, Imamura M, Taraseviciene-Stewart L, Walker LA*, et al* (2008). Involvement of RhoA/Rho kinase signaling in protection against monocrotaline-induced pulmonary hypertension in pneumonectomized rats by dehydroepiandrosterone. *Am J Physiol Lung Cell Mol Physiol* **295**(1): L71-78.

Horton JD (2002). Sterol regulatory element-binding proteins: transcriptional activators of lipid synthesis. *Biochem Soc Trans* **30**(Pt 6): 1091-1095.

Indolfi C, Di Lorenzo E, Perrino C, Stingone AM, Curcio A, Torella D*, et al* (2002). Hydroxymethylglutaryl coenzyme A reductase inhibitor simvastatin prevents cardiac hypertrophy induced by pressure overload and inhibits p21ras activation. *Circulation* **106**(16): 2118-2124.

Jones P, Kafonek S, Laurora I, Hunninghake D (1998). Comparative dose efficacy study of atorvastatin versus simvastatin, pravastatin, lovastatin, and fluvastatin in patients with hypercholesterolemia (the CURVES study). *Am J Cardiol* **81**(5): 582-587.

Kilic FS, Ozatik Y, Kaygisiz B, Baydemir C, Erol K (2012). Acute antidepressant and anxiolytic effects of simvastatin and its mechanisms in rats. *Neurosciences (Riyadh)* **17**(1): 39-43.

LaBar KS, Cabeza R (2006). Cognitive neuroscience of emotional memory. *Nat Rev Neurosci* **7**(1): 54-64.

Li L, Zhang S, Zhang X, Li T, Tang Y, Liu H*, et al* (2013). Autophagy enhancer carbamazepine alleviates memory deficits and cerebral amyloid-beta pathology in a mouse model of Alzheimer's disease. *Curr Alzheimer Res* **10**(4): 433-441.

Lin MT, Lujan R, Watanabe M, Adelman JP, Maylie J (2008). SK2 channel plasticity contributes to LTP at Schaffer collateral-CA1 synapses. *Nat Neurosci* **11**(2): 170-177.

Lingor P, Teusch N, Schwarz K, Mueller R, Mack H, Bahr M*, et al* (2007). Inhibition of Rho kinase (ROCK) increases neurite outgrowth on chondroitin sulphate proteoglycan in vitro and axonal regeneration in the adult optic nerve in vivo. *J Neurochem* **103**(1): 181-189.

Lowry OH, Rosebrough NJ, Farr AL, Randall RJ (1951). Protein measurement with the Folin phenol reagent. *J Biol Chem* **193**(1): 265-275.

Marz P, Otten U, Miserez AR (2007). Statins induce differentiation and cell death in neurons and astroglia. *Glia* **55**(1): 1-12.

Mathew SJ, Coplan JD, Gorman JM (2001). Neurobiological mechanisms of social anxiety disorder. *Am J Psychiatry* **158**(10): 1558-1567.

Matthews RT, Yang L, Browne S, Baik M, Beal MF (1998). Coenzyme Q10 administration increases brain mitochondrial concentrations and exerts neuroprotective effects. *Proc Natl Acad Sci U S A* **95**(15): 8892-8897.

Mazzucchelli C, Brambilla R (2000). Ras-related and MAPK signalling in neuronal plasticity and memory formation. *Cell Mol Life Sci* **57**(4): 604-611.

Mereu G, Fa M, Ferraro L, Cagiano R, Antonelli T, Tattoli M*, et al* (2003). Prenatal exposure to a cannabinoid agonist produces memory deficits linked to dysfunction in hippocampal long-term potentiation and glutamate release. *Proc Natl Acad Sci U S A* **100**(8): 4915-4920.

Ming XF, Viswambharan H, Barandier C, Ruffieux J, Kaibuchi K, Rusconi S*, et al* (2002). Rho GTPase/Rho kinase negatively regulates endothelial nitric oxide synthase phosphorylation through the inhibition of protein kinase B/Akt in human endothelial cells. *Mol Cell Biol* **22**(24): 8467-8477.

Mohamed A, Saavedra L, Di Pardo A, Sipione S, Posse de Chaves E (2012). beta-amyloid inhibits protein prenylation and induces cholesterol sequestration by impairing SREBP-2 cleavage. *J Neurosci* **32**(19): 6490-6500.

Moreno S, Mugnaini E, Ceru MP (1995). Immunocytochemical localization of catalase in the central nervous system of the rat. *J Histochem Cytochem* **43**(12): 1253-1267.

Oh JE, Karlmark Raja K, Shin JH, Pollak A, Hengstschlager M, Lubec G (2006). Cytoskeleton changes following differentiation of N1E-115 neuroblastoma cell line. *Amino Acids* **31**(3): 289-298.

Opazo P, Watabe AM, Grant SG, O'Dell TJ (2003). Phosphatidylinositol 3-kinase regulates the induction of long-term potentiation through extracellular signal-related kinase-independent mechanisms. *J Neurosci* **23**(9): 3679-3688.

Pallottini V, Martini C, Cavallini G, Bergamini E, Mustard KJ, Hardie DG*, et al* (2007). Age-related HMG-CoA reductase deregulation depends on ROS-induced p38 activation. *Mech Ageing Dev* **128**(11-12): 688-695.

Pallottini V, Montanari L, Cavallini G, Bergamini E, Gori Z, Trentalance A (2004). Mechanisms underlying the impaired regulation of 3-hydroxy-3-methylglutaryl coenzyme A reductase in aged rat liver. *Mech Ageing Dev* **125**(9): 633-639.

Panksepp J, Siviy S, Normansell L (1984). The psychobiology of play: theoretical and methodological perspectives. *Neurosci Biobehav Rev* **8**(4): 465-492.

Papakostas GI, Ongur D, Iosifescu DV, Mischoulon D, Fava M (2004). Cholesterol in mood and anxiety disorders: review of the literature and new hypotheses. *Eur Neuropsychopharmacol* **14**(2): 135-142.

Parikh A, Childress C, Deitrick K, Lin Q, Rukstalis D, Yang W (2010). Statin-induced autophagy by inhibition of geranylgeranyl biosynthesis in prostate cancer PC3 cells. *Prostate* **70**(9): 971-981.

Pellow S, Chopin P, File SE, Briley M (1985). Validation of open:closed arm entries in an elevated plus-maze as a measure of anxiety in the rat. *J Neurosci Methods* **14**(3): 149-167.

Pellow S, File SE (1986). Anxiolytic and anxiogenic drug effects on exploratory activity in an elevated plus-maze: a novel test of anxiety in the rat. *Pharmacol Biochem Behav* **24**(3): 525-529.

Peter H, Hand I, Hohagen F, Koenig A, Mindermann O, Oeder F, *et al* (2002). Serum cholesterol level comparison: control subjects, anxiety disorder patients, and obsessive-compulsive disorder patients. *Can J Psychiatry* **47**(6): 557-561.

Pfrieger FW (2003). Role of cholesterol in synapse formation and function. *Biochim Biophys Acta* **1610**(2): 271-280.

Pinheiro SH, Zangrossi H, Jr., Del-Ben CM, Graeff FG (2007). Elevated mazes as animal models of anxiety: effects of serotonergic agents. *An Acad Bras Cienc* **79**(1): 71-85.

Popjak G, Edmond J, Anet FA, Easton NR, Jr. (1977). Carbon-13 NMR studies on cholesterol biosynthesized from [13C]mevalonates. *J Am Chem Soc* **99**(3): 931-935.

Ramakers GM, Storm JF (2002). A postsynaptic transient K(+) current modulated by arachidonic acid regulates synaptic integration and threshold for LTP induction in hippocampal pyramidal cells. *Proc Natl Acad Sci U S A* **99**(15): 10144-10149.

Reitz C, Luchsinger J, Tang MX, Manly J, Mayeux R (2005). Impact of plasma lipids and time on memory performance in healthy elderly without dementia. *Neurology* **64**(8): 1378-1383.

Rex CS, Chen LY, Sharma A, Liu J, Babayan AH, Gall CM, *et al* (2009). Different Rho GTPase-dependent signaling pathways initiate sequential steps in the consolidation of long-term potentiation. *J Cell Biol* **186**(1): 85-97.

Saheki A, Terasaki T, Tamai I, Tsuji A (1994). In vivo and in vitro blood-brain barrier transport of 3-hydroxy-3-methylglutaryl coenzyme A (HMG-CoA) reductase inhibitors. *Pharm Res* **11**(2): 305-311.

Seasholtz TM, Majumdar M, Brown JH (1999). Rho as a mediator of G protein-coupled receptor signaling. *Mol Pharmacol* **55**(6): 949-956.

Segatto M, Di Giovanni AL, Marino M, Pallottini V (2013). Analysis of the protein network of cholesterol homeostasis in different brain regions: an age and sex dependent perspective. *J Cell Physiol*.

Segatto M, Trapani L, Marino M, Pallottini V (2011). Age- and sex-related differences in extra-hepatic low-density lipoprotein receptor. *J Cell Physiol* **226**(10): 2610-2616.

Sierra S, Ramos MC, Molina P, Esteo C, Vazquez JA, Burgos JS (2011). Statins as neuroprotectants: a comparative in vitro study of lipophilicity, blood-brain-barrier penetration, lowering of brain cholesterol, and decrease of neuron cell death. *J Alzheimers Dis* **23**(2): 307-318.

Silva AJ, Kogan JH, Frankland PW, Kida S (1998). CREB and memory. *Annu Rev Neurosci* **21**: 127-148.

Sui L, Wang J, Li BM (2008). Role of the phosphoinositide 3-kinase-Akt-mammalian target of the rapamycin signaling pathway in long-term potentiation and trace fear conditioning memory in rat medial prefrontal cortex. *Learn Mem* **15**(10): 762-776.

Tang PH, Miles MV, DeGrauw A, Hershey A, Pesce A (2001). HPLC analysis of reduced and oxidized coenzyme Q(10) in human plasma. *Clin Chem* **47**(2): 256-265.

Taylor AE, Guthrie PA, Smith GD, Golding J, Sattar N, Hingorani AD*, et al* (2011). IQ, educational attainment, memory and plasma lipids: associations with apolipoprotein E genotype in 5995 children. *Biol Psychiatry* **70**(2): 152-158.

Tong XK, Lecrux C, Rosa-Neto P, Hamel E (2012). Age-dependent rescue by simvastatin of Alzheimer's disease cerebrovascular and memory deficits. *J Neurosci* **32**(14): 4705-4715.

Trapani L, Melli L, Segatto M, Trezza V, Campolongo P, Jozwiak A*, et al* (2011a). Effects of myosin heavy chain (MHC) plasticity induced by HMGCoA-reductase inhibition on skeletal muscle functions. *FASEB J* **25**(11): 4037-4047.

Trapani L, Segatto M, Ascenzi P, Pallottini V (2011b). Potential role of nonstatin cholesterol lowering agents. *IUBMB Life* **63**(11): 964-971.

Trezza V, Baarendse PJ, Vanderschuren LJ (2009). Prosocial effects of nicotine and ethanol in adolescent rats through partially dissociable neurobehavioral mechanisms. *Neuropsychopharmacology* **34**(12): 2560-2573.

Trezza V, Baarendse PJ, Vanderschuren LJ (2010). The pleasures of play: pharmacological insights into social reward mechanisms. *Trends Pharmacol Sci* **31**(10): 463-469.

Trezza V, Campolongo P, Cassano T, Macheda T, Dipasquale P, Carratu MR*, et al* (2008). Effects of perinatal exposure to delta-9-tetrahydrocannabinol on the emotional reactivity of the offspring: a longitudinal behavioral study in Wistar rats. *Psychopharmacology (Berl)* **198**(4): 529-537.

Wang Q, Tang XN, Wang L, Yenari MA, Ying W, Goh BC*, et al* (2006). Effects of high dose of simvastatin on levels of dopamine and its reuptake in prefrontal cortex and striatum among SD rats. *Neurosci Lett* **408**(3): 189-193.

Wei YM, Li X, Xu M, Abais JM, Chen Y, Riebling CR*, et al* (2013). Enhancement of autophagy by simvastatin through inhibition of Rac1-mTOR signaling pathway in coronary arterial myocytes. *Cell Physiol Biochem* **31**(6): 925-937.

While A, Keen L (2010). The effects of statins on mood: a review of the literature. *Eur J Cardiovasc Nurs* **11**(1): 85-96.

Whitton P, Curzon G (1990). Anxiogenic-like effect of infusing 1-(3-chlorophenyl) piperazine (mCPP) into the hippocampus. *Psychopharmacology (Berl)* **100**(1): 138-140.

Table 1. Effect of simvastatin on lipid composition of selected brain regions. Number of rats contributing to each value are shown in brackets.

	Cholesterol (mg/g tissue)	Dolichol (µg/g tissue)	CoQ9 (µg/g tissue)	CoQ10 (µg/g tissue)	
Amygdala	31.77 ± 9.36	1.37 ± 0.16	3.13 ± 0.36	1.72 ± 0.16	Veh (4)
	30.45 ± 9.81	1.55 ± 0.17	3.28 ± 0.70	1.75 ± 0.33	Sim (4)
Hippocampus	32.05 ± 6.47	1.47 ± 0.29	3.39 ± 0.07	1.77 ± 0.08	Veh (5)
	34.15 ± 10.65	1.46 ± 0.13	3.40 ± 0.19	1.91 ± 0.07	Sim (5)
Prefrontal cortex	29.47 ± 9.82	1.35 ± 0.18	3.11 ± 0.29	1.56 ± 0.14	Veh (5)
	31.76 ± 5.18	1.46 ± 0.17	3.48 ± 0.17	1.75 ± 0.08	Sim (5)
Dorsal striatum	34.49 ± 2.16	1.48 ± 0.05	3.58 ± 0.32	1.64 ± 0.17	Veh (5)
	31.81 ± 2.83	1.46 ± 0.13	4.23 ± 0.24	1.85 ± 0.11	Sim (5)
Ventral striatum	27.42 ± 1.93	1.32 ± 0.06	2.80 ± 0.70	1.26 ± 0.32	Veh (4)
	28.36 ± 5.06	1.46 ± 0.25	3.05 ± 0.76	1.38 ± 0.36	Sim (4)

Figure legends

Figure 1. Effects of chronic simvastatin treatment in the social interaction, elevated plus maze and inhibitory avoidance tests.

Simvastatin treatment (1.5 mg/kg per day; *i.p.*) reduced the total time spent in active social interaction (**a**). No statistically significant difference was found in **b**) the percentage of time spent in the open arms, **c**) the percentage of open entries and in **d**) the total arm entries evaluated in the elevated plus maze test. Simvastatin treatment **e**) had no effects on the approach latency in the acquisition trial of the inhibitory avoidance task, whereas **f**) enhanced twenty-four-hour avoidance latencies in the retention trial. **g**) No statistically significance difference was found between simvastatin-treated rats and their controls in response to shock delivered during the acquisition trial of the inhibitory avoidance test. Data represent mean values ± SEM. *$p < 0.05$, ***$p < 0.001$ vs. control ($n = 10$-11 per treatment group). Veh = vehicle-treated rats. Sim = simvastatin-treated rats.

Figure 2. Efficacy of HMGR inhibition by simvastatin and effects on neuronal and astrocytic content in different brain regions.

a) Representative Western blot and densitometric analysis of nSREBP-2 in amygdala (Am), hippocampus (Hp), prefrontal cortex, dorsal striatum and ventral striatum. **b**) Representative Western blot and densitometric analysis of LDLr in amygdala (Am), hippocampus (Hp), prefrontal cortex, dorsal striatum and ventral striatum. **c**) Representative Western blot and densitometric analysis of the neuronal marker NeuN in amygdala (Am), hippocampus (Hp), prefrontal cortex, dorsal striatum and ventral striatum. **d**) Representative Western blot and densitometric analysis of the astrocytic marker GFAP in amygdala (Am), hippocampus (Hp), prefrontal cortex, dorsal striatum and ventral striatum. Protein levels were normalized with α-tubulin. The data are

expressed as arbitrary units obtained by analyzing the protein bands with ImageJ software for Windows, for details see the main text. All the results obtained are presented as the mean ± S.D. *p < 0.05, **p < 0.01; Student's t test with respect to the control group of the same brain region analyzed. n = 6 animals/group. Veh = vehicle-treated rats. Sim = simvastatin-treated rats.

Figure 3. Effect of HMGR inhibition on Rab3 membrane localization and degradation in different brain regions.

a) Representative Western blot and densitometric analysis of Rab3 in preparations of synaptic vesicle membranes from amygdala (Am), hippocampus (Hp), prefrontal cortex, dorsal striatum and ventral striatum. Rab3 active fraction was expressed as the membrane:cytosol ratio.

Data are represented as arbitrary units obtained by analyzing the protein bands with ImageJ software for Windows, for details see the main text. All the results are expressed as the mean ± S.D. *p < 0.05 and **p < 0.01; Student's t test with respect to the control group of the same brain region analyzed. n = 6 animals/group. Veh = vehicle-treated rats. Sim = simvastatin-treated rats.

b) Representative Western blot obtained by Rab3 degradation assay in cytosolic fractions from amygdala, hippocampus, prefrontal cortex, dorsal striatum and ventral striatum. The time course analysis was performed at 0, 1, 2, 4, 8, 16 and 24 hours. The results are represented as arbitrary units obtained by evaluating the protein bands with ImageJ software for Windows, for details see the main text. n = 6 animals/group. Veh = vehicle-treated rats. Sim = simvastatin-treated rats.

Figure 4. Effect of HMGR inhibition by simvastatin on Ras, RhoA membrane localization and Akt activation in different brain regions.

a) Representative Western blot and densitometric analysis of Ras in amygdala (Am), hippocampus (Hp), prefrontal cortex, dorsal striatum and ventral striatum. Ras active fraction was expressed as the membrane:cytosol ratio. **b**) Representative Western blot and densitometric analysis of RhoA in

amygdala (Am), hippocampus (Hp), prefrontal cortex, dorsal striatum and ventral striatum. RhoA active fraction was expressed as the membrane:cytosol ratio. **c)** Representative Western blot and densitometric analysis of Akt phosphorylation/activation in amygdala (Am), hippocampus (Hp), prefrontal cortex, dorsal striatum and ventral striatum. Protein levels were normalized with α-tubulin. The results are represented as arbitrary units obtained by analyzing the protein bands with ImageJ software for Windows, for details see the main text. All the data are expressed as the mean ± S.D. *$p < 0.05$; Student's t test with respect to the control group of the same brain region analyzed. $n = 6$ animals/group. Veh = vehicle-treated rats. Sim = simvastatin-treated rats.

Figure 5. Akt phosphorylation and the consequent CREB activation are dependent on RhoA/ROCK pathway.

a) Representative Western blot and densitometric analysis of RhoA in primary hippocampal neurons. RhoA active fraction was expressed as the membrane:cytosol ratio. All the data are expressed as arbitrary units obtained by analyzing the protein bands with ImageJ software for Windows, for details see the main text. **b)** Representative Western blot and densitometric analysis of Akt phosphorylation/activation in primary hippocampal neurons. p-Akt protein levels were normalized with total Akt levels and α-tubulin. **c)** Representative Western blot and densitometric analysis of CREB phosphorylation/activation in primary hippocampal neurons. p-CREB protein levels were normalized with total CREB levels and α-tubulin. All the data are expressed as arbitrary units obtained by evaluating the protein bands with ImageJ software for Windows, for details see the main text. All the results represent the mean ± S.D of at least three different experiments. *$p < 0.05$, **$p < 0.01$, and ***$p < 0.001$determined using one-way ANOVA followed by Dunnett post-test. Veh = vehicle; Sim = simvastatin; MVA = mevalonate; GG = geranylgeraniol; HF = hydroxyfasudil.

Figure 6. p-CREB and PSD-95 distribution in hippocampus of simvastatin- and vehicle-treated rats.

(a) Overview of p-CREB immunohistochemistry in a sagittal section of rat brain. Hippocampal formation showed higher positivity in the nucleus of pyramidal cells in CA1-CA3 fields and of granule cells in DG. Mossy cells in the hylus were especially immunoreactive.

b) Overview of PSD-95 immunohistochemistry in a sagittal section of rat brain showing immunopositivity localized to pyramidal cell layer of CA1-CA3, to granule neurons of DG, and to hylar mossy neurons.

Hp, hippocampus; Or, stratum oriens; Pyr, stratum pyramidale; Rad, stratum radiatum; GL, granule cell layer; PoDG, polymorphic layer; ML, molecular layer.
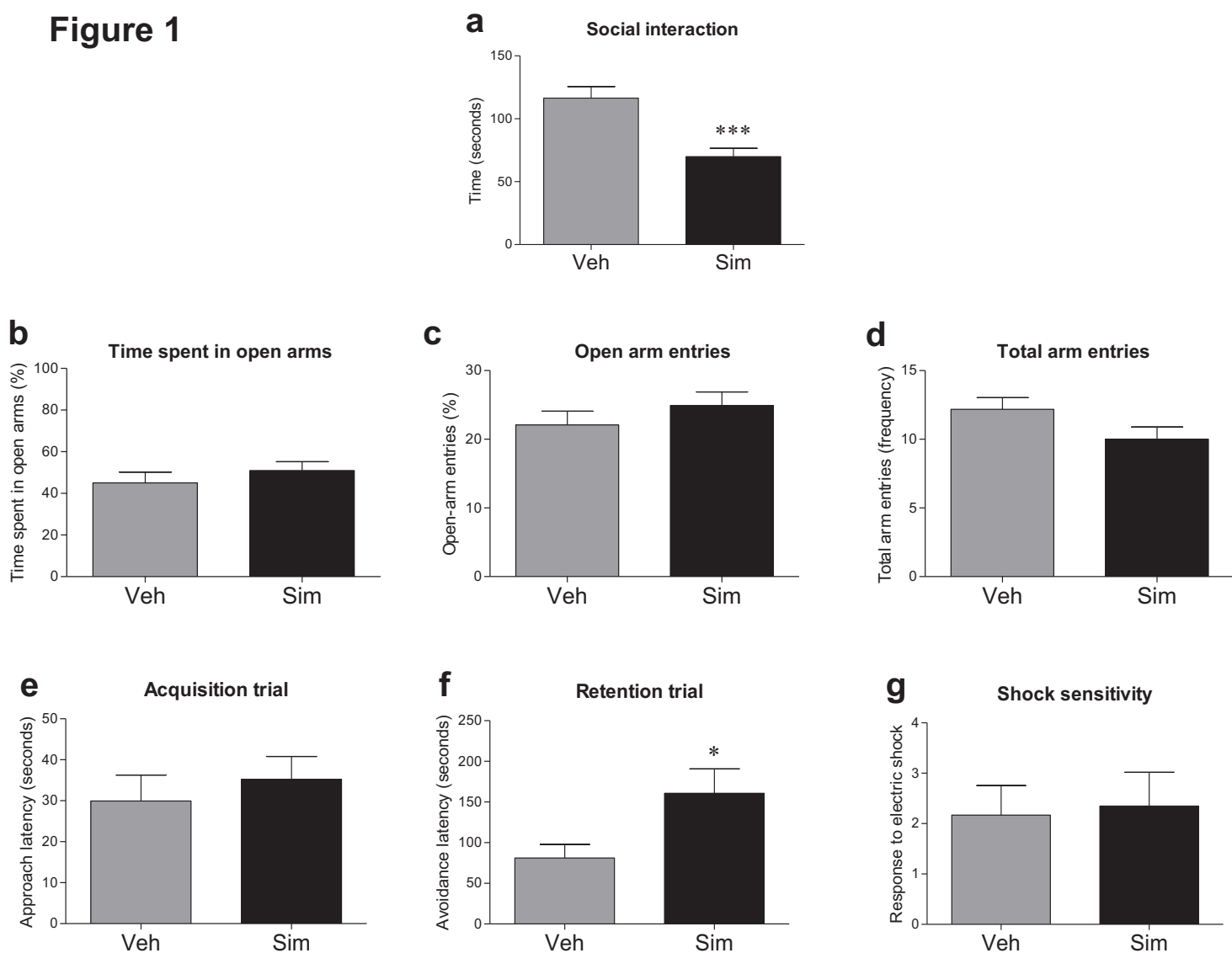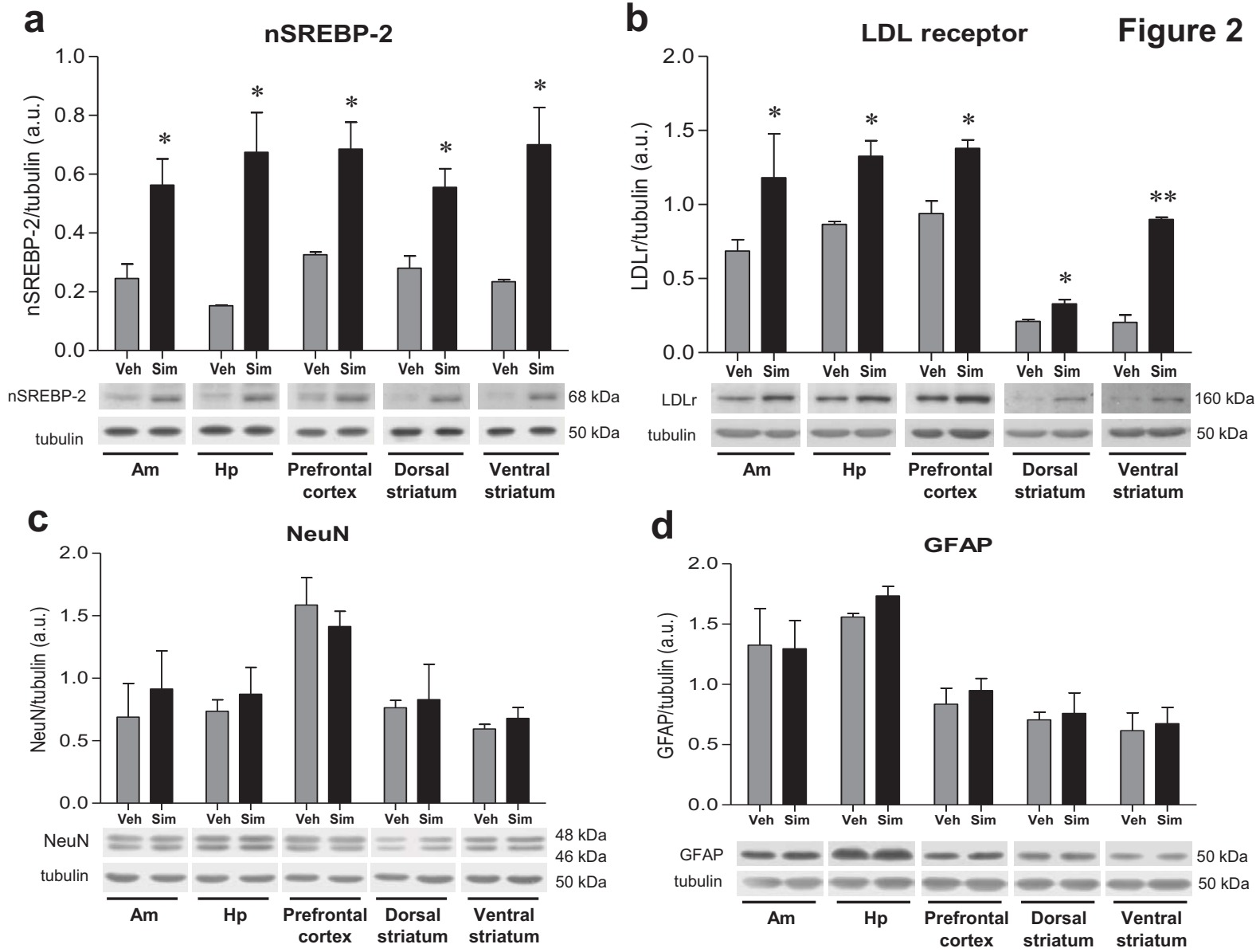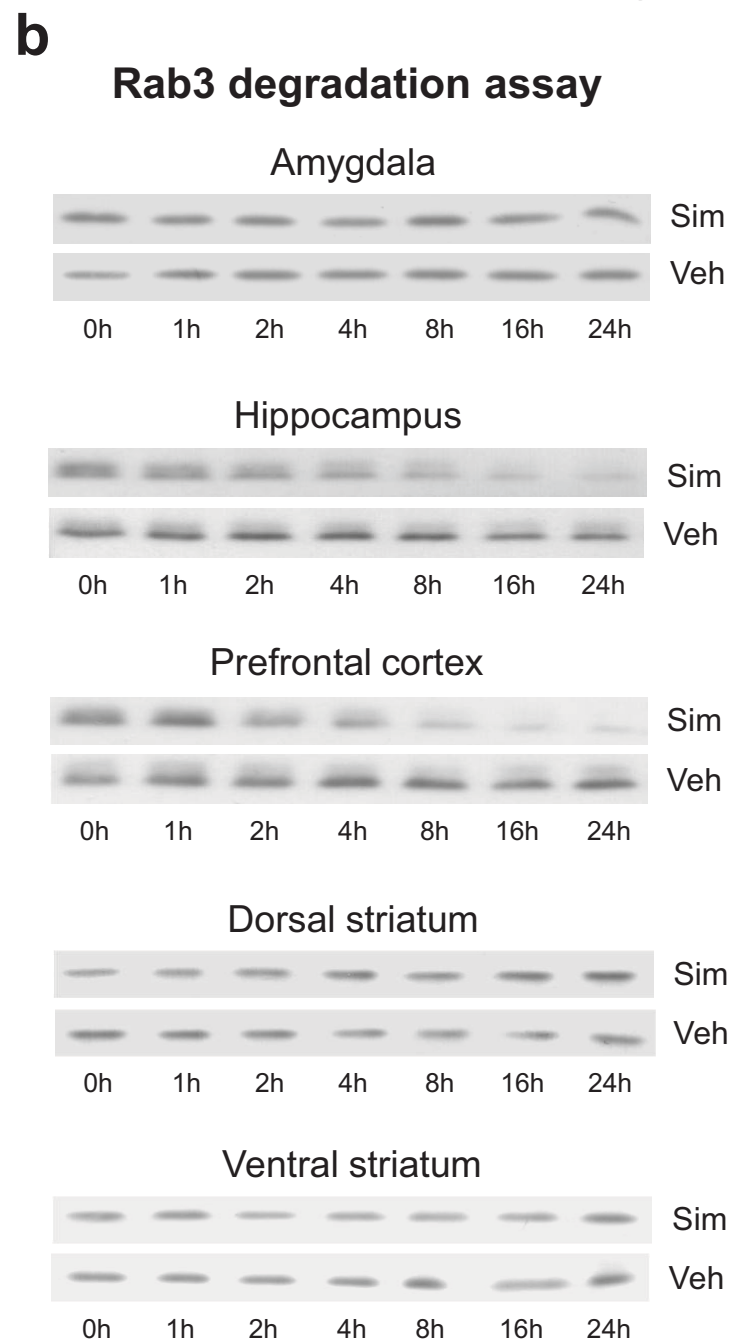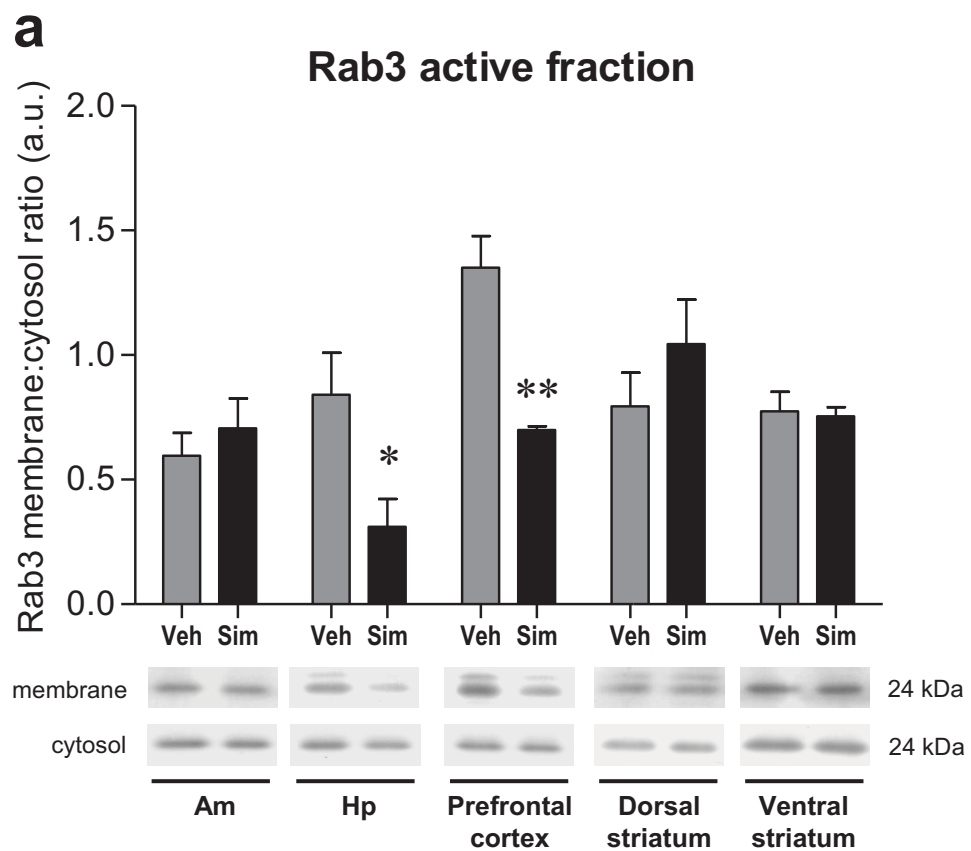
Figure 1

Figure 2

Figure 3

a Rab3 active fraction

b Rab3 degradation assay

Figure 4

a

Ras active fraction

Ras membrane:cytosol ratio (a.u.)

membrane — 21 kDa
cytosol — 21 kDa

Am   Hp   Prefrontal cortex   Dorsal striatum   Ventral striatum

b

RhoA active fraction

RhoA membrane:cytosol ratio (a.u.)

membrane — 24 kDa
cytosol — 24 kDa

Am   Hp   Prefrontal cortex   Dorsal striatum   Ventral striatum

c

Akt activation state

p-Akt / t-Akt / tubulin (a.u.)

p-Akt — 60 kDa
t-Akt — 60 kDa
tubulin — 50 kDa

Am   Hp   Prefrontal cortex   Dorsal striatum   Ventral striatum

Figure 5

a

RhoA active fraction

b

Akt activation state

c

CREB activation state

A p-CREB   **B** PSD95

vehicle   simvastatin   vehicle   simvastatin

Hp

CA1 — Or, Pyr, Rad

CA3 — Rad, Pyr, Or

DG — PoDG, GL, ML